

# Mechatronic design of a 3-DOF parallel translational manipulator

Paolo Righettini, Alessandro Tasora, Hermes Giberti

Polytechnic of Milan

Department of Electrical Engineering

P.zza L. da Vinci 32, Italy, 20133 Milano

paolo.righettini@polimi.it, tasora@mech.polimi.it, giberti@mech.polimi.it

**Abstract:** This paper presents the development steps of a fast manipulator, up to the building of the experimental device, in a context of mechatronic design which implies the integration of several engineering disciplines. High performance of the manipulator has been achieved by means of the suitable integration of the mechanical part and the drive part. For the mechanical part we choose a 3-dof parallel translational solution that allows high stiffness, low weight and low dynamic forces, mostly because of the closed loop chains implied by their structure. For the drive part we adopted brushless motors that show high dynamic performance and high efficiency. The design of the manipulator, as well as the selection of transmissions and motors, has been carried out by means of a multibody software that implements specific features aimed at the simulation of the mechanical behaviour of robotic devices.

KEYWORDS: parallel manipulator, mechatronic design, motor selection

## 1 INTRODUCTION

In general, parallel kinematics offers the advantage of high stiffness/weight ratio when compared to serial robots. Moreover, some specific architectures of parallel robots exploit pure 3-DOF translation of the end-effector, thus suggesting their adoption in applications where simple but fast manipulations of objects must be performed, like in assembly lines or in pick-and-place tasks.

In order to develop a parallel robotic device which must operate at high speed, special care must be taken in the design of truss, joints, transmissions and actuators.

We developed specific simulation software tools which helped us in the mechatronic design of a fast parallel manipulator, targeting at the optimal utilization of the three brushless motors. In detail, by using a custom multibody software, we were able to test many different configurations of motor/reducers for trajectories representing typical pick-and-place tasks of the end-effector.

The final design of our robot exploits a light moving structure and linear actuators based on prismatic guides and custom ball-screws transmissions, for sake of least inertia and good precision. In the meanwhile, special care was taken in avoiding some typical pitfalls of other

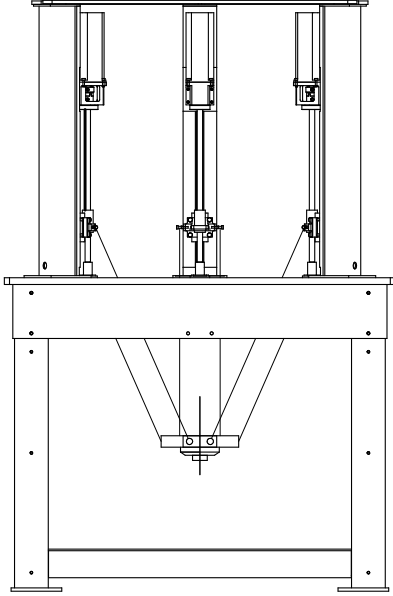


Figure 1: Kinematic structure of the robot, using six linkages and twelve spherical joints

parallel-translational robots, such as the low torsional stiffness and joint backlash.

On the basis of these considerations, a final prototype has been built, and experimental tests on its performance are currently performed.

Motion control of manipulator and high-level programming are handled by a PC platform, running a real-time operating system based on Linux.

## 2 KINEMATICS

The proposed parallel manipulator, whose scheme is presented in figure 1, is made of three linear bearings which slide on vertical ground-fixed guides, each of them connected to the end-effector by means of two inextensible parallel shafts with spherical joints on both ends; this structure has three translational degrees of freedom [1]. The couple of inextensible parallel shafts with spherical joints on both ends realizes a double universal

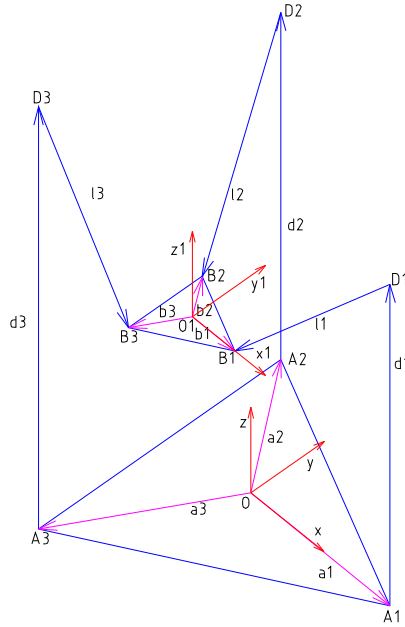


Figure 2: Parameters for kinematics

joint constrain and therefore this manipulator is of type 3-PUU.

With the above assumptions on pure translation of the end effector, we can easily write the equations for the direct and inverse kinematics of the robot, using a geometric approach. Considering the geometric parameters of figure 2, we can write the three vectorial closure equations that lead to the analytical form of the inverse kinematics [7]:

$$d_i = p_z \pm \left[ -\vec{e}_i^2 - p_x^2 - \dots \dots p_y^2 + 2e_{ix}p_x + 2e_{iy}p_y + \vec{l}_i^2 \right]^{1/2} \quad (1)$$

where  $\vec{e}_i = \vec{a}_i - \vec{b}_i$ , and  $d_i$  is the joint-coordinate of the  $i$ -th linear actuator as a function of the cartesian position of the end-effector  $\vec{p}_i$ .

This equation may be used in the control program of the robot to project on-line the coordinates of the end-effector's space to the coordinates of joint's space.

The direct kinematics couldn't be eas-

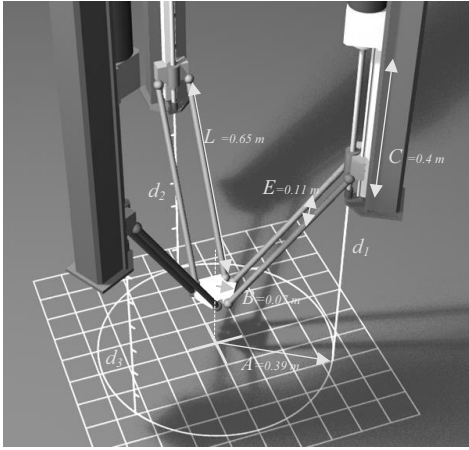


Figure 3: Multibody model of the robot used for simulations, with main measures

ily determined in analytical form, so it is computed as well as the dynamics by means of a multibody program [5].

### 3 DESIGN AND OPTIMIZATION

In order to choose the dimensions of the linkages and the stroke of the actuators it is necessary to find a good compromise between wide working volume and manipulator stiffness [4].

Therefore we developed a *Javascript* program, running as a client of our multibody software *CHRONO*, which optimized the geometry of our robot trying to achieve good dynamical performances in the entire working volume. For this purpose the tool studies the jacobian matrix  $[J]$  of the IK/FK coordinate transformations over the entire working volume, as depicted in figure 4. Since the growth of the condition number of  $[J]$  can be considered a reliable warning of how much the robot is near a singular configuration [3], our optimization tool used this criteria to find the best measures for the robot.

We found that, for sliding bearings with a maximum clearance of  $C =$

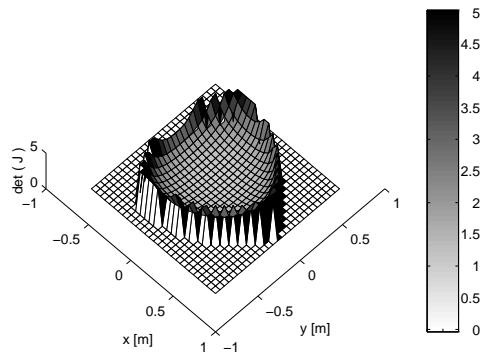


Figure 4: Jacobian in XY plane

400 mm , we get a good working volume and satisfactory dynamic properties with rod lengths  $L = 650$  mm and robot radius  $A = 390$  mm, as shown in figure 3.

The final working volume is very wide but oddly shaped, so the effective working volume is deliberately limited by a cylinder with a diameter of 400 mm and height of 200 mm.

The dynamic performances of the robot have been analyzed taking into account the mass characteristics of the transmission (ball screws and pads of the caged ball linear guides) and the limits of both brushless motors and motor's electronic drives.

The choice of the motor and the reduction ratio of the transmission has been carried out by means of a selection procedure based on the motion requested at the end-effector. Briefly, under the hypothesis that the load is totally dynamic the equilibrium between the motor, neglecting the efficiency of the transmission and the load is expressed by the equation

$$T_m = \left( \frac{J_m}{\tau} + \tau J_l \right) \dot{\omega}_l \quad (2)$$

where the subscripts  $m$  and  $l$  respec-

tively indicate a motor's property and a load property,  $T$  represents the motor's torque,  $\tau$  is the generalized transmission ratio and  $\dot{\omega}_l$  in the acceleration requested to the load. Using the transmission ratio  $\tau_o = \sqrt{J_m/J_l}$  that maximize the load's acceleration, from the equation (2) a suitable motor must satisfy the equation

$$\frac{T_m}{\sqrt{J_m}} \geq 2\sqrt{J_l}\dot{\omega}_l. \quad (3)$$

The first term of this equation depends on the motor's characteristics that satisfy the load's requests represented by the second term of the equation. For the motor selection this equation must be satisfied for both the peak conditions of the load and the root mean square of the load, index of the motor's heating. The latter condition therefore must be satisfied by the nominal torque of the motor  $T_{m_N}$  and leads to the equation

$$\frac{T_{m_N}}{\sqrt{J_m}} \geq 2\sqrt{J_l}\dot{\omega}_{l_{RMS}}. \quad (4)$$

The maximum velocity of the motor must satisfy the maximum velocity requested by the load. For a transmission ratio  $\tau_o$ , this condition leads to

$$\tau_o\omega_{m_{MAX}} \geq \omega_{l_{MAX}} \quad (5)$$

The equations (3), (4) and (5) may be respectively expressed in the form

$$\begin{aligned} F_{m_P} &\geq 2F_{l_P} \\ F_{m_{RMS}} &\geq 2F_{l_{RMS}} \\ E_m &\geq E_l \end{aligned} \quad (6)$$

where  $F_{m_P} = \frac{T_{m_{MAX}}}{\sqrt{J_m}}$  depends on both the motor and the motor's drive characteristics.

These equations drive the choice of the motor by means of the diagram in figure 5 that represents both the motor performances  $F_{m_{RMS}}$  and  $E_m$ , and the load requests  $2F_{l_P}$  and  $2F_{l_{RMS}}$ . Selecting the

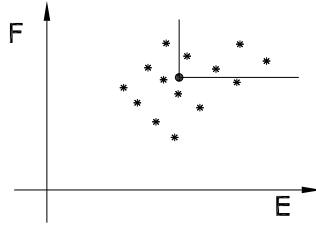


Figure 5: E-F diagram

suitable motor with the minimum possible nominal torque we may determinate the transmission ratio  $\tau_o = \sqrt{J_l/J_m}$  that maximize the load's acceleration; from the transmission catalogue we will select the transmission more close to  $\tau_o$ .

For the parallel manipulator presented in this paper, the selection procedure leads to a brushless motor with  $T_{m_N} = 2.5$  Nm,  $T_{m_P} = 5$  Nm,  $\omega_{m_{MAX}} = 4500$  rpm and a ball screw with pitch of 32 mm and diameter of 16 mm.

#### 4 EXPERIMENTAL DEVICE

While designing the pieces for the prototype, special care has been put in creating light moving parts. In this way we could meet the requirements of low inertia, as suggested by dynamical analysis performed with multibody simulations.

We were able to design a light end effector, entirely made of Ergal alloy, whose weight is less than 1.4 kg including the six linkages. Such linkages are made of empty tubes with high radius (to avoid flexional vibrations) and thin section (1 mm, enough for axial loads).

From our past experience with other parallel robots, we know that joint clearances can be major causes of bad precision, so we spent some efforts in finding high-precision ball joints and linear guides, yet choosing the solution with the lowest mass. Either the linear guides and screws have recirculating spheres,

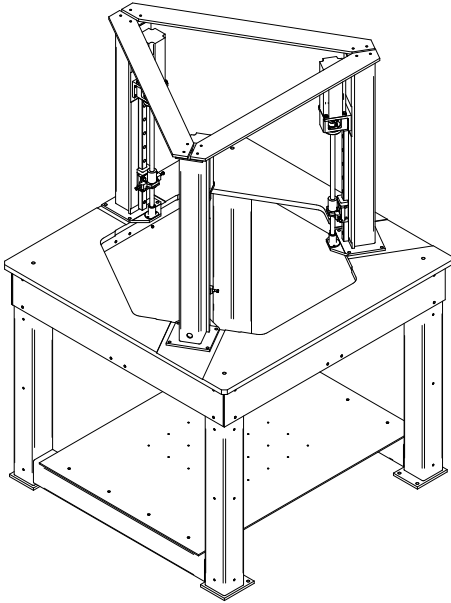


Figure 6: Assembly of the robot, with truss and base

for maximum precision and no stick-slip effects, see figure 8.

The truss is made of a welded table support and three vertical struts, see figure 6. This modular solution has been designed to be as stiff as possible.

The linear actuator module, shown in figure 7, uses a compact coupling between motor and screw thanks to light Oldham joint with low inertia and zero torsional clearance.

Each brushless motor has a digital driver which performs the speed control loop. The position control loop is performed by a PC computer with Linux RT (an hard real-time release of Linux) embodying a multi-channel AD/DA board, which reads the encoder positions and outputs the analog setpoints for the three motor drivers.

After some experimental tests, the prototype showed the same performances that we expected from early simulations. The speed during pick-and-

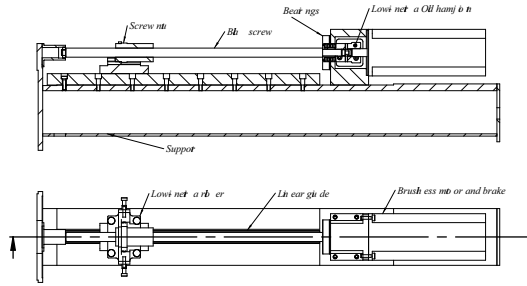


Figure 7: Detail of linear actuator with ball screw

place operations is very high: more than 5 cycles/second, with trajectories of 200 mm. Precision is good even while following fast trajectories (average  $\varepsilon < 0.5mm$ ), and becomes higher during slow or steady motions ( $\varepsilon < 0.1mm$ ), as in the figures 9 and 10.

## 5 CONCLUSION

We developed a parallel robotic device which operates at high speed, either because of an accurate layout of the actuators, either by virtue of an optimized design of truss, joints and transmissions in sake of the highest stiffness with the least inertia.

For this purpose we implemented special features in our multibody simulation software, which assisted us in the design

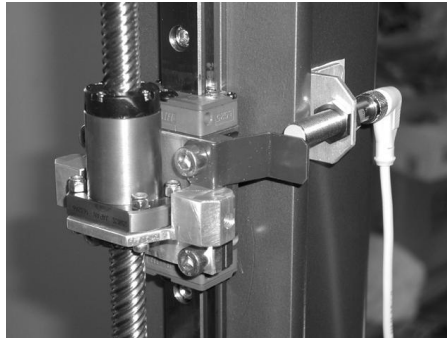


Figure 8: Detail of low-inertia roller

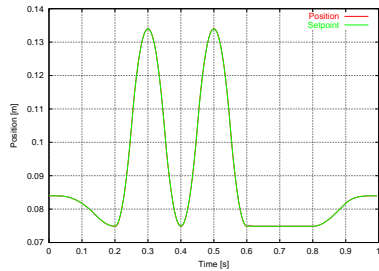


Figure 9: Position and set-point of an axis

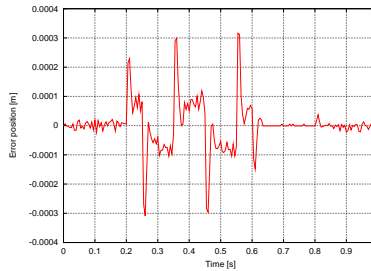


Figure 10: Error position of figure 9

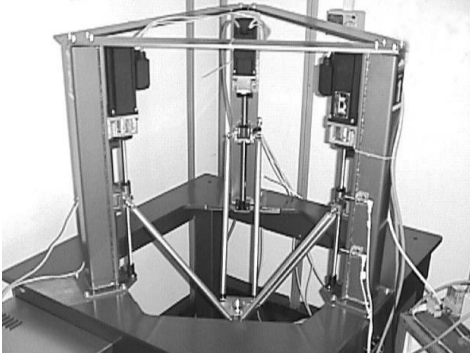


Figure 11: Experimental device

process. By performing repeated simulations, we were able to find the optimal choice in terms of motor and screw transmission.

The robot prototype shows great dynamical properties, being able to perform more than five “U” trajectories ( $s=200\text{mm}$ ,  $h=50\text{mm}$ ) per second, with high precision and low vibrations.

On the basis of these experimental results, we believe that this robot can represent a satisfactory proposal for applications of fast packaging and fast assembly.

## REFERENCES

- [1] R.Clavel, M.Bouri, S.Grousset, M.Thurneyssen, *A new 4 D.O.F. parallel robot: the Manta*, The International Workshop on Parallel Kinematics Machines, UCIMU, Milano 1999.
- [2] R.Di Gregorio, V.Parenti-Castelli, *Mobility analysis of the 3-UPU parallel mechanism assembled for a pure translational motion*, IEEE-ASME International Conference on Advanced Intelligent Mechatronics (AIM'99), Atlanta 1999.
- [3] M.H.Perng, T.C.Lee, Y.S.Tsai, *A systematic design procedure for parallel machine tools regarding mechanical efficiency, stiffness and workspace*, The International Workshop on Parallel Kinematics Machines, UCIMU, Milano 1999.
- [4] D.N.Centea, F.Audren, H.Lacheray, R.Teltz, *Optimization of the TIARA hexapod design -A machine tool based on parallel kinematic structures-*, The International Workshop on Parallel Kinematics Machines, UCIMU, Milano 1999.
- [5] A.Tasora, *An optimized lagrangian multiplier approach for interactive multibody simulation in kinematic and dynamical digital prototyping*, VII ISCSB, Milano, 2001.
- [6] [www.rtlinux.org](http://www.rtlinux.org), Official Realtime Linux web site, 2001.
- [7] A. Tasora, H. Giberti, P. Righettini, *Design and experimental test of a pneumatic translational 3dof parallel manipulator*, 10th International Workshop on robotics in Alpe-Adria-Danube region RAAD-2001, May 16-18 2001, Vienna, Austria.